Journal of Research in Pharmacy

Research Article

www.jrespharm.com

QSAR and pharmacophore models for screening anti-inflammatory activity among substituted (pyrrolo[1,2-*a*][1,2,4]triazino[2,3-*c*]quinazoline-5*a*-yl)carboxylic acids

Viktor STAVYTSKYI [1], Oleksii ANTYPENKO [1*], Oleg DEVINYAK [2], Oleksii VOSKOBOİNİK [1], Sergiy KOVALENKO [1]

[1] Department of Organic and Bioorganic Chemistry, Zaporizhzhia State Medical University, Mayakovsky Ave. 26, 69035, Zaporizhzhia, Ukraine.

[2] Department of Pharmaceutical disciplines, Uzhhorod National University, Narodna Square, 3, 88000, Uzhhorod, Transcarpathian region, Ukraine.

* Corresponding Author. E-mail: antypenkoan@gmail.com (O.M.); Tel. +380-066-965 87 52.

Received: 04 January 2022 / Revised: 10 June 2022 / Accepted: 10 June 2022

ABSTRACT: This study is devoted to the development of QSAR and pharmacophore models for screening of anti-inflammatory activity among substituted (pyrrolo[1,2-*a*][1,2,4]triazino[2,3-*c*]quinazoline-5*a*-yl)carboxylic acids, obtained in earlier research of our scientist group. Genetic algorithm–multiple linear regression allowed to calculate two three-parameter QSAR equations for each model of experimental inflammation. It was found that the anti-inflammatory activity in the "carrageenan" model depends on the descriptors GATS5m and B10[C-O] and the presence in the structure nROH functional group. Whereas, in the "formalin" model, pharmacological effect is determined by the descriptors E2p, R2e+, F09[N-F], that reveal positive contribution to the anti-inflammatory activity. The obtained equations are characterized by significant predictive power and are determined by both internal and external validation. The parameters of prognostic ability, namely the values of the cross-validation Q^2_{LOO} coefficient, are 0.8509 and 0.7653 respectively. Using pharmacophore modeling, it was found that substituted (pyrrolo[1,2-*a*][1,2,4]triazino[2,3-*c*]quinazoline-5*a*-yl)carboxylic acids bind with potential biotargets through the carboxyl moiety at the 5a position (potential participant in the formation of hydrogen bonds), regardless of the model of experimental inflammation. Additional factors influencing activity are electron withdrawing substituents, namely aromatic (fluorophenyl) cycle at the certain distance and oxygen at the second position in the molecule. The aforesaid shows the prospects for further structural modification of the molecule by replacing the triazole ring with azole one or by removing it while retaining the noted pharmacophore fragments. It is important that the developed models complement each other and can later be used for virtual screening of anti-inflammatory activity among quinazolines and its condensed analogues.

KEYWORDS: Pyrrolo[1,2-*a*][1,2,4]triazino[2,3-*c*]quinazolines; anti-inflammatory activity; QSAR- and pharmacophoric models; screening.

1. INTRODUCTION

Quinazolines and their condensed analogues are a known group of biologically active compounds with diverse biological activity and significant potential for targeted search for active pharmaceutical ingredients. This class of compounds is characterized by anti-inflammatory, analgesic, hypoglycemic, diuretic, anticonvulsant, antitumor, antiviral, antitubercular, antimalarial, antibacterial and other activities [1-13]. It should be noted, that quinazolines are widely used in medical practice as antitumor ("Gefitinib", "Erlotinib", "Vandetanib", "Lapatinib", "Dacomitinib", "Afatinib", "Trimetrexate" and others), hypotensive ("Prazosin", "Doxazosin"), hypoglycemic ("Linagliptin"), diuretics ("Metolazone","Quinetazone"), anti-inflammatory ("Proquison"), antiviral, antibacterial drugs [10, 12, 14]. Thanks to the introduction and usage of innovative technologies, it is now established that this class of tyrosine kinase (TK), serine-threonine kinase (STK), dual TK-histone deacetylases (HDACs) inhibitors, tumor necrosis factor-α (TNF-α), phosphodiesterase (PDE10A), dehydrofolate reductase receptors, as well as p53 regulators, α_1-adrenergic receptor blockers, antagonizing Melanin-concentrating hormone receptor 1 (MCHR1), etc. [1, 3, 7-11]. Information on the structures of receptors, as well as receptor-ligand interactions (homologous models, structural information based on X-ray diffraction and NMR analysis, thermodynamics of ligand binding, effects of point mutations, dynamic

How to cite this article: Stavytskyi V, Antypenko O, Devinyak D, Voskoboinik O, Kovalenko S. QSAR and pharmacophore models for screening anti-inflammatory activity among substituted (pyrrolo[1,2-a][1,2,4]triazino[2,3-c]quinazoline-5a-yl)carboxylic acids. J Res Pharm. 2022; 26(5): 1420-1431.

ISSN: 2630-6344

http://dx.doi.org/10.29228/jrp.235

movements of receptor and ligands, etc.) allowed the use at the present stage of drug search "*de novo design*" methods [15].

These methods not only reduced the time required to search for APIs with a certain type of activity, but also the time it takes to enter the market. For example, the active pharmaceutical ingredient (DSP-1181) for the treatment of mental disorders (obsessive-compulsive disorder) was created in collaboration with the British startup Exscientia and the Japanese pharmaceutical company Sumitomo Dainippon Pharma (artificial intelligence solved the problem for 12 months) [16]. Executive Director of Exscientia, Professor Andrew Hopkins called it "a key milestone in drug invention".

Given the above arguments, to find potential "hit compounds" as objects for further structural modification, we used the methods of computer chemistry to obtain preliminary hypotheses about the mechanisms of anti-inflammatory activity, structural requirements for active compounds, and model development for further virtual screening. Previously, based on drug-design methods, we structurally modeled and synthesized a new class of pyrrolo[1,2-*a*][1,2,4]triazino[2,3-*c*]quinazolines as potential anti-inflammatory agents [17, 18]. Given that QSAR and pharmacophore modeling have proven to be good approaches for quantitative study of the general chemical properties of a large number of compounds, we have developed, optimized and validated them, screened the collection of chemical compounds for these models and analyzed the screening results. QSAR is one of the major computational molecular modeling methodologies that together with other *in silico* methods could reduce the high cost of experimental synthesis. That's why it definitely worthies of attention.

Therefore, the aim of the work was to develop QSAR- and pharmacophore models among pyrrolo[1,2-*a*][1,2,4]triazino[2,3-*c*]quinazolines on the basis of the obtained experimental data of anti-inflammatory activity. And further evaluation of obtained models for their usage in targeted search of new drugs.

2. RESULTS AND DISCUSSION

Two QSAR equations 1.1 and 1.2 were obtained in the process of calculation using the compounds of the training and prediction set. To build them, we have used a genetic algorithm, taking into account the large number of descriptors that were obtained by Dragon software. Analysis of the contributions of each allows us to compare the effectiveness of molecular descriptors in assessing the activity of the studied compounds. In order to avoid data overload, we focused on the development of simple models, with the possibility of further analysis of the model on an external test set. In addition, multiple line-by-regression was chosen to provide clear and realistic QSAR equations.

Equation 1.1: Anti-inflammatory activity, % ("carrageenan" edema) = -59.6939(±28.1405)**GATS5m**+52.1582(±10.519)**nROH**-16.4232(±10.8175)**B10[C-O]**+75.1782(±28.5634), (n=24, R^2 = 0.8949; s = 7.4445; F = 39.7387; p = 0.0001; RMSEtr = 6.5654; R^2cv (Q^2loo) 0.8509; R^2-R^2cv 0.0441; RMSEcv 7.8214; MAEcv 6.1097; PRESScv 1101.1505; CCCcv 0.9212; RMSEex 14.5196; MAEex 10.9673; PRESSext 1264.9081);

Equation 1.2: Anti-inflammatory activity, % ("formalin" edema) = 461.0349(±148.8201)**E2p**+203.8143(±163.6924)**R2e+**22.5011(±10.563)**F09[N-F]**-135.616(±48.3742), (n=24, R^2 = 0.8419; s = 8.4633; F = 24.8593; p = 0.0001; RMSEtr = 7.4640; R^2cv (Q^2loo) 0.7653; R^2-R^2cv 0.0767; RMSEcv 9.0956; MAEcv 7.4201; PRESScv 1489.1383; CCCcv 0.8733; RMSEex 17.7625; MAEex 14.5007; PRESSext 1893.0438).

Values and characteristics of molecular descriptors that were used to build QSAR models are shown in tables 1 and 2.

Table 1. Characteristics of molecular descriptors selected for the construction of QSAR equations

Name	Block	Description
GATS5m	2D autocorrelations	Geary autocorrelation of lag 5 weighted by mass
nROH	number of hydroxyl groups	functional group counts
B10[C-O]	presence/absence of C - O at topological distance 10	2D Atom Pairs
E2p	2nd component accessibility directional WHIM index / weighted by polarizability	WHIM descriptors
R2e+	R maximal autocorrelation of lag 2 / weighted by Sanderson electronegativity	GETAWAY descriptors
F09[N-F]	Frequency of N - F at topological distance 9	2D Atom Pairs

Table 2. The values for selected molecular descriptors present in QSAR models.

Compound	GATS5m	nROH	B10[C-O]	E2p	R2e+	F09[N-F]
2.1	1.073	1	0	0.381	0.127	0
2.2	1.168	1	1	0.349	0.145	0
2.3	1.077	1	1	0.348	0.145	0
2.4	0.898	1	1	0.330	0.139	0
2.5	0.918	1	1	0.331	0.147	0
2.6	0.717	1	1	0.358	0.072	0
2.7	0.718	1	1	0.402	0.075	0
2.8	1.192	1	1	0.335	0.118	0
2.9	0.863	1	1	0.345	0.119	1
2.10	0.823	1	1	0.332	0.137	1
2.11	0.766	1	1	0.349	0.138	1
2.12	0.823	1	1	0.293	0.109	1
2.13	0.859	1	0	0.409	0.123	0
2.14	0.985	1	1	0.337	0.120	0
2.15	0.949	1	1	0.372	0.080	0
2.16	0.779	1	1	0.321	0.116	0
2.17	0.820	1	1	0.345	0.116	0
2.18	0.741	1	1	0.302	0.107	1
2.19	0.799	1	1	0.309	0.097	1
2.20	0.671	1	1	0.327	0.115	1
2.21	0.738	1	1	0.368	0.109	1
2.22	1.005	0	0	0.336	0.071	0
2.23	0.869	0	1	0.288	0.060	0
2.24	0.680	0	1	0.264	0.055	1

Interpretation of the "carrageenan" equation 1.1, which contains 2D autocorrelation indices GATS5m and B10[C-O] indicates that the presence of terminal atoms with high atomic masses at topological distance 5 and the presence of a pair of C-O atoms at topological distance 10 in the studied substances corresponds to a decrease in anti-inflammatory activity. However, a significant increase in anti-inflammatory activity will be observed in the presence of the nROH functional group (carboxyl fragment) in the structures [19, 20]. In the "formalin" equation 1.2, the descriptors F09[N-F], E2p and R2e+, make only a positive contribution to anti-inflammatory activity. It is important that the presence of the descriptor F09[N-F] at the topological distance 9 indicates the possibility of additional donor-acceptor interactions of fluorine atoms with substrates [21] and significantly affects the electronegativity and polarizability of the molecule (Table 2). This is clearly demonstrated by experimental studies and predicted activity (Tables 3, 4, 6).

Validation of equations in order to confirm their predictive ability was carried out using a prediction set (external) and training set (internal). First, the descriptors were calculated for each structure, using the QSAR equation then the activity values were calculated and compared with the already known experimental values. Cross-sleep validation was performed by the "leave-one-out" method. The optimal equation is one in which the standard error is minimal. For predictive power of the QSAR equations additional parameters were calculated and could be found in Tables 3, 4.

Table 3. Statistic details regarding QSAR equation of carrageenan-induced edema.

Compound	Exp. endpoint	Pred. by model eq.	Pred.Mod. Eq.Res	Pred. LOO	Pred. LOO Res.	HAT i/i (h*=0.6667)	Std.Pred. Mod.Eq. Res.	Std.Pred. LOO Res.
2.1[a]	57.90	63.2848	5.3848	66.7925	8.8925	0.3945	0.9295	1.5350
2.2[a]	40.81	41.1908	0.3808	41.3692	0.5592	0.3190	0.0620	0.0910
2.3[b]	75.77	46.6229	-29.1471	-	-	0.1860	-4.3396	-4.3396
2.4[a]	64.72	57.3081	-7.4119	56.712	-8.008	0.0744	-1.0349	-1.1181
2.5[a]	54.92	56.1143	1.1943	56.2139	1.2939	0.0770	0.1670	0.1809
2.6[a]	63.80	68.1127	4.3127	68.9589	5.1589	0.1640	0.6336	0.7579
2.7[b]	58.54	68.0530	9.5130	-	-	0.1630	1.3967	1.3967
2.8[a]	44.66	39.7581	-4.9019	36.9682	-7.6918	0.3627	-0.8248	-1.2943
2.9[b]	63.02	59.3974	-3.6226	-	-	0.0759	-0.5062	-0.5062
2.10[a]	74.60	61.7852	-12.8148	60.5661	-14.0339	0.0869	-1.8014	-1.9728
2.11[b]	69.23	65.1877	-4.0423	-	-	0.1197	-0.5787	-0.5787
2.12[a]	51.37	61.7852	10.4152	62.7759	11.4059	0.0869	1.4641	1.6033
2.13[a]	81.46	76.0593	-5.4007	71.7315	-9.7285	0.4449	-0.9737	-1.7539
2.14[a]	50.40	52.1148	1.7148	52.3134	1.9134	0.1038	0.2433	0.2715
2.15[a]	50.27	54.2637	3.9937	54.6393	4.3693	0.0860	0.5611	0.6139
2.16[a]	60.46	64.4117	3.9517	64.9022	4.4422	0.1104	0.5628	0.6327
2.17[a]	49.95	61.9643	12.0143	63.1248	13.1748	0.0881	1.6900	1.8532
2.18[b]	69.15	66.6801	-2.4699	-	-	0.1404	-0.3579	-0.3579
2.19[a]	63.25	63.2178	-0.0322	63.2143	-0.0357	0.0982	-0.0046	-0.0050
2.20[b]	53.85	70.8587	17.0087	-	-	0.2192	2.5857	2.5857
2.21[a]	79.66	66.8592	-12.8008	64.7199	-14.9401	0.1432	-1.8576	-2.1681
2.22[a]	15.17	15.1858	0.0158	15.2041	0.0341	0.5364	0.0031	0.0067
2.23[a]	8.15	6.8810	-1.2690	6.0712	-2.0788	0.3896	-0.2182	-0.3574
2.24[a]	16.91	18.1632	1.2532	19.1245	2.2145	0.4341	0.2238	0.3954

[a] training set.
[b] prediction set.

Table 4. Statistic details regarding QSAR equation of formalin-induced edema.

Compound	Exp. endpoint	Pred. by model eq.	Pred.Mod .Eq.Res.	Pred. LOO	Pred. LOO Res.	HAT i/i (h*=0.6667)	Std.Pred. Mod.Eq. Res.	Std.Pred. LOO Res.
2.1[a]	53.76	65.9227	12.1627	68.1232	14.3632	0.1532	1.5617	1.8443
2.2[a]	70.18	54.8382	-15.3418	51.7107	-18.4693	0.1693	-1.9889	-2.3944
2.3[b]	59.52	54.3772	-5.1428	-	-	0.1707	-0.6673	-0.6673
2.4[a]	49.42	44.8557	-4.5643	43.8307	-5.5893	0.1834	-0.5968	-0.7308
2.5[a]	46.74	46.9472	0.2072	47.0086	0.2686	0.2285	0.0279	0.0361
2.6[a]	46.01	44.1091	-1.9009	43.5361	-2.4739	0.2316	-0.2562	-0.3335
2.7[b]	45.93	65.0061	19.0761	-	-	0.4967	3.1770	3.1770
2.8[a]	34.60	42.8807	8.2807	43.7342	9.1342	0.0934	1.0276	1.1335
2.9[b]	64.30	70.1960	5.8960	-	-	0.2639	0.8120	0.8120
2.10[a]	60.31	67.8712	7.5612	70.9879	10.6779	0.2919	1.0617	1.4993
2.11[b]	64.38	75.9127	11.5327	-	-	0.3267	1.6606	1.6606
2.12[a]	46.21	44.1841	-2.0259	43.5438	-2.6662	0.2401	-0.2746	-0.3614
2.13[a]	84.05	78.0164	-6.0336	75.1943	-8.8557	0.3187	-0.8637	-1.2677
2.14[a]	32.33	44.2104	11.8804	45.4399	13.1099	0.0938	1.4746	1.6272

2.15[a]	61.73	52.1941	-9.5359	49.1736	-12.5564	0.2406	-1.2929	-1.7025
2.16[a]	42.69	36.0186	-6.6714	35.0453	-7.6447	0.1273	-0.8438	-0.9669
2.17[a]	43.19	47.0835	3.8935	47.4208	4.2308	0.0797	0.4796	0.5211
2.18[b]	82.98	47.9258	-35.0542	-	-	0.2143	-4.6726	-4.6726
2.19[a]	54.33	49.1149	-5.2151	47.7964	-6.5336	0.2018	-0.6897	-0.8641
2.20[b]	50.78	61.0822	10.3022	-	-	0.218	1.3766	1.3766
2.21[a]	79.05	78.7617	-0.2883	78.5814	-0.4686	0.3848	-0.0434	-0.0706
2.22[a]	23.60	33.7625	10.1625	36.1326	12.5326	0.1891	1.3335	1.6444
2.23[a]	11.93	9.3909	-2.5391	7.9985	-3.9315	0.3542	-0.3733	-0.5780
2.24[a]	19.84	19.8081	-0.0319	19.7851	-0.0549	0.4186	-0.0049	-0.0085

[a] training set.
[b] prediction set.

Graphs of comparison of predicted and experimental activity values for training and prediction sets of compounds are presented in Figure 1. The predictive ability of the calculated equations was tested using the prediction set and quantified by the value of the cross-validation coefficient Q^2_{LOO}. For equations 1.1 and 1.2, the Q^2_{LOO} values were 0.8509 and 0.7653, respectively. Thus, it can be considered that the obtained models are characterized by significant predictive value, determined by both internal and external validation, and can be used for virtual screening of anti-inflammatory activity of substances of this class of compounds.

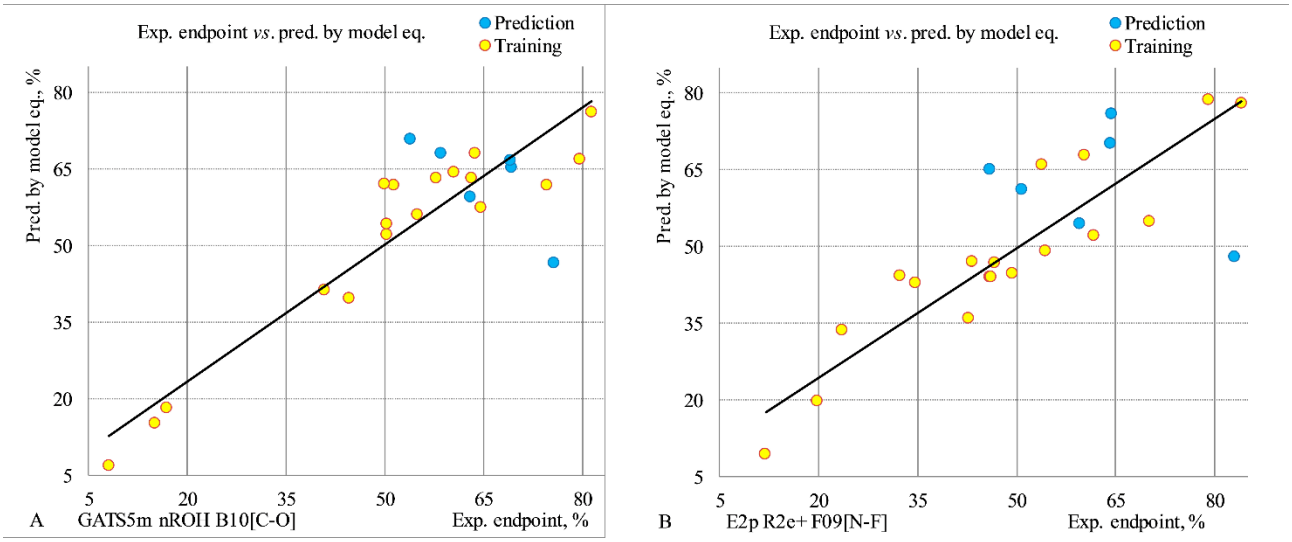

Figure 1. Graph of experimental and predicted data of the percentage of anti-inflammatory activity on the carrageenan-induced (A, equation 1.1.) and formalin-induced (B, equation 1.2) models: training set - yellow, prediction set – blue.

The method of pharmacophore modeling was also used to increase the efficiency of design and search for new potential "hit compounds" with anti-inflammatory activity among substituted of pyrrolo[1,2-*a*]azolo-(azino-)[*c*]quinazoline. Moreover, in the QSAR equations descriptors are present that are calculated from the spatial coordinates of the molecule's atoms in the selected conformation and compare three-dimensional molecular geometry with the molecular influence matrix and with the relationship of atoms by molecular topology. This model makes it possible to correlate the activity with the spatial arrangement of different pharmacophores. To successfully find the active compounds, the sets of steric and electronic features of the compounds are taken into account, that are necessary for their optimal interaction with the molecular target.

The pharmacophore modeling on the carrageenan model revealed three variants of pharmacophore with the same accuracy, but different sets of pharmacophore centers and different degrees of mutual overlap of active compounds (Table 5). For these models, the virtual enrichment factor (enrichment factor - calculated on the basis of available data) is 1.55. All formed pharmacophore models are five-component and indicate the predominant role of compounds as acceptors of the hydrogen atom in the formation of hydrogen bonds with biotarget. For model 1.1 with the best degree of overlap of active compounds, the geometric structure of the pharmacophore in three projections is derived (Figure 2). The diameter of the pharmacophore model 1.1

(maximum distance between pharmacophore centers) is 10.11 Å, with the most distant pharmacophore groups being the projections of the donor and the hydrogen bond acceptor, which are located on opposite edges. Both projections of hydrogen bond acceptors are located close to each other at a distance of 1.57 Å. The close location of these projections may indicate the formation of only one hydrogen bond in this position when the ligand interacts with the biotarget, stabilized by two possible variants of the hydrogen acceptor.

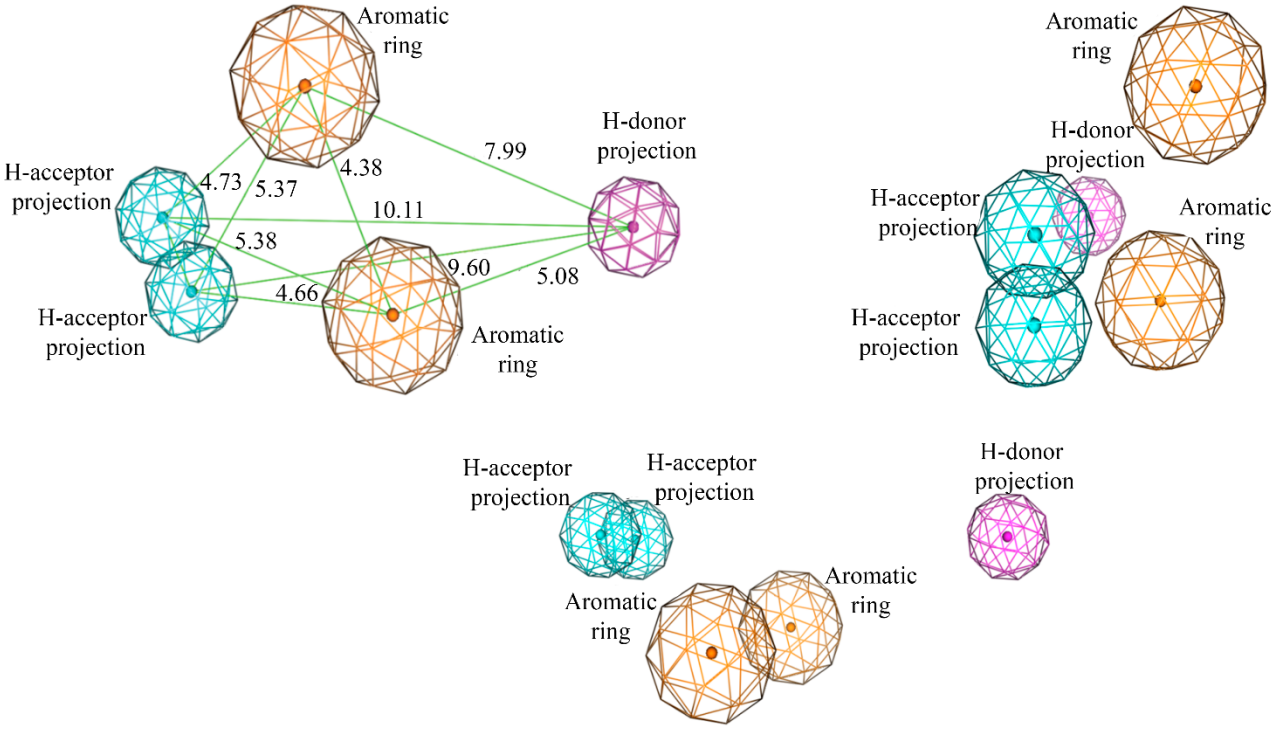

Figure 2. Geometry of the pharmacophore model 1.1 responsible for the manifestation of anti-inflammatory activity in the carrageenan model, among the substituted pyrrolo[1,2-*a*][1,2,4]triazino[2,3-*c*]quinazolines (distance in Å).

Analysis of the coordination of active substances with the pharmacophore model highlights the key role of one of the nitrogen atoms of the triazine ring and oxo group in the 2nd position of this cycle as hydrogen acceptors in the interaction with biotargeting, and indicates participation of the carboxyl group in interaction (Figure 3). In this case, the pharmacophore model identifies the carboxyl group as a potential participant in the formation of hydrogen bonds. However, it is known that under the conditions of the biological environment, the carboxyl group can dissociate and be in the form of an anion. The pharmacophore model 1.1 still captures the same spatial arrangement of carboxyl groups in the active substances. Thus, the model assumes the possibility of the carboxyl group to participate in the interaction not only in the dissociated state, but also in the form of an anion.

Pharmacophore modeling in formalin-induced edema revealed one variant of pharmacophore with an accuracy of 89.3% (model 2.1) and two variants with an accuracy of 85.7% (models 2.2 and 2.3, Table 5). Both model 2.1 and model 2.2 contain the same set of pharmacophore centers, but with different locations and different degrees of overlap of the active compounds. In the case of virtual screening, the enrichment factor (calculated based on available data) is 1.73. Model 2.1 shows the geometric structure of the pharmacophore in three projections (Figure 4). The diameter of the pharmacophore model 2.1 (maximum distance between pharmacophore centers) is 9.51 Å, with the most distant pharmacophore groups are projections of the donor and acceptor of hydrogen bonds, which are located on opposite edges. Both projections of hydrogen bond acceptors are located close to each other at a distance of 0.99 Å. The close location of these projections also indicates the formation in this position of only one hydrogen bond in the interaction of the ligand with the biotarget, stabilized by two possible variants of the hydrogen acceptor.

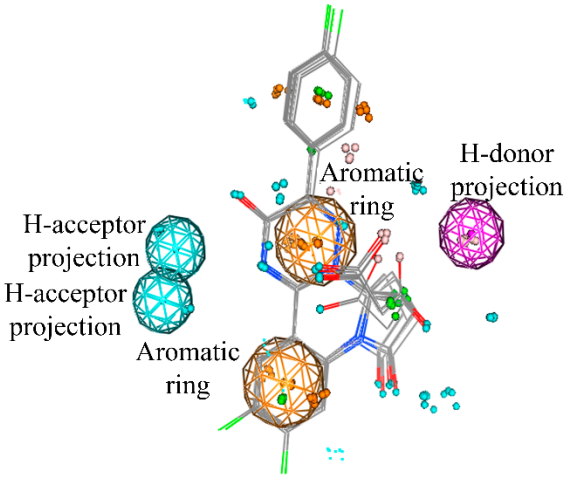

Figure 3. Compounds with expressed anti-inflammatory activity among substituted pyrrolo[1,2-*a*][1,2,4]triazino[2,3-*c*]quinazolines (4, 7) in a conformation consistent with pharmacophore model 1.1.

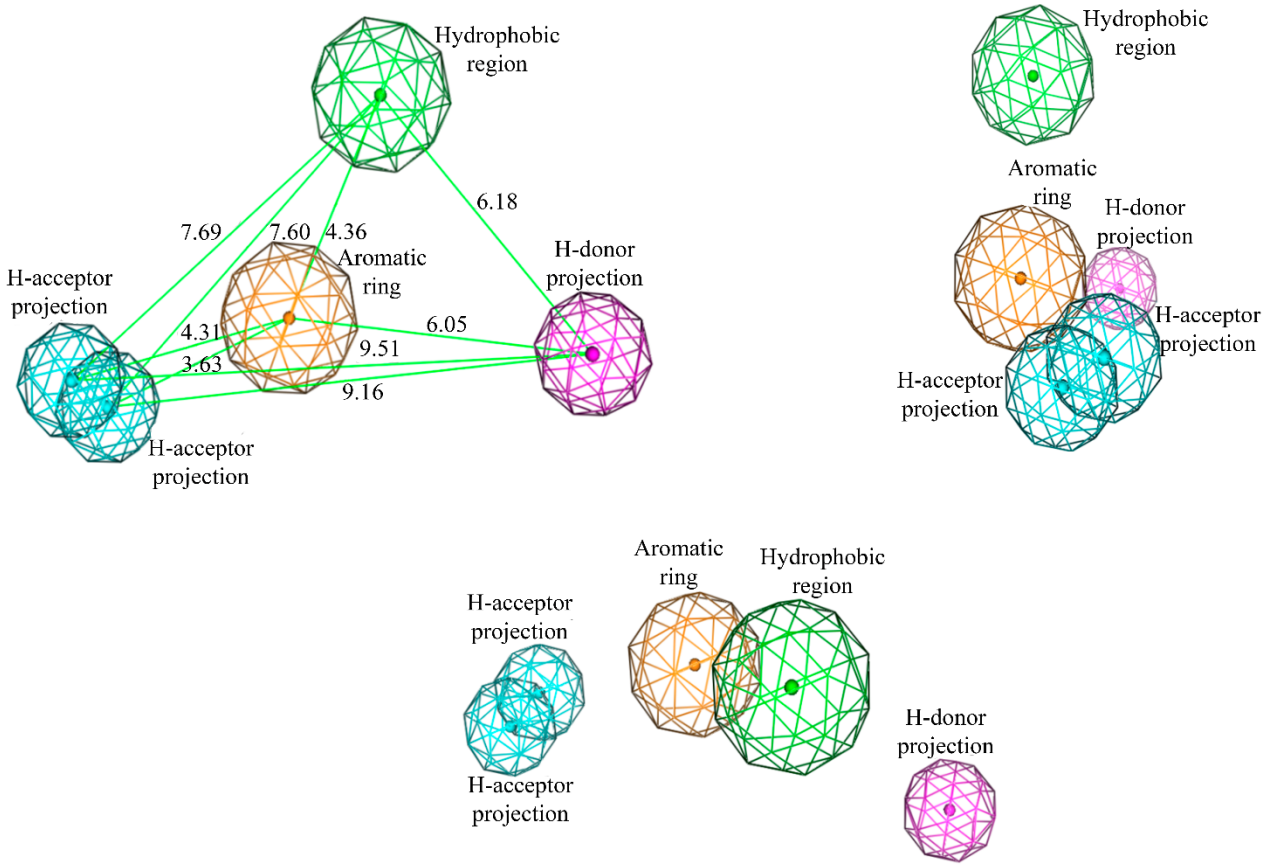

Figure 4. Geometry of the pharmacophore model 2.1 responsible for the manifestation of anti-inflammatory activity on the formalin model, among the substituted pyrrolo[1,2-*a*][1,2,4]triazino[2,3-*c*]quinazolines (distance in Å).

The analysis of the coordination of active substances with the pharmacophore model 2.1 repeats the general picture of model 1.1, indicating the participation of one of the nitrogen atoms of the triazine ring and oxo group in the 2nd position of this cycle as hydrogen acceptors in interaction with biotarget. Also, carboxyl groups are probably involved in the interaction with biotarget (Figure 5). The main features of model 2.1 coincide with the characteristics of model 1.1. This is an expected result, because the same type of biological activity is modeled on the same database of substances.

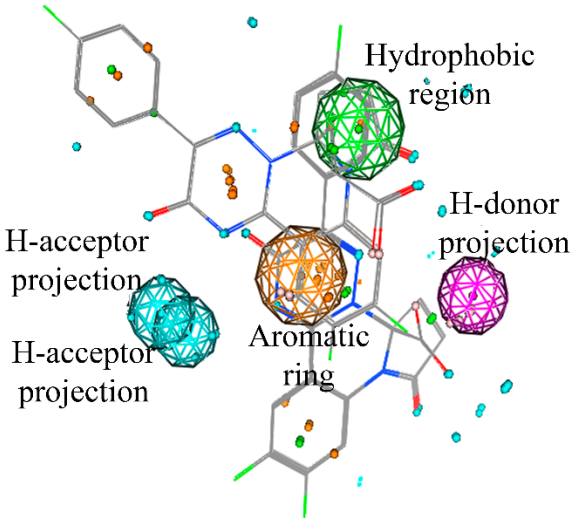

Figure 5. Compounds with expressed anti-inflammatory activity among substituted pyrrolo[1,2-*a*][1,2,4]triazino [2,3-*c*]quinazolines (4, 7) in a conformation consistent with pharmacophore model 2.1.

Table 5. Characteristics of pharmacophore models for detection and screening of anti-inflammatory activity.

№ of model	Number of pharmacophore centers	List of pharmacophore centers	The degree of mutual overlap of active compounds	Precision classification, %
		Carrageenan-induced edema		
model 1.1	5	Two aromatic cycles (or cycles with π-bonds), a hydrogen bond donor projection and two hydrogen bond acceptor projections	10.34	78.6
model 1.2	5	Aromatic cycle (or π-bond cycle), hydrogen bond donor projection and three hydrogen bond acceptor projections	8.77	78.6
model 1.3	5	Hydrophobic region and four projections of the hydrogen bond acceptor	6.86	78.6
		Formalin-induced edema		
model 2.1	5	Aromatic cycle (or cycle with π-bonds), hydrophobic region, hydrogen donor projection and two hydrogen acceptor projections	8.93	89.3
model 2.2	5	Aromatic cycle (or cycle with π-bonds), hydrophobic region, hydrogen donor projection and two hydrogen acceptor projections	12.51	85.7
model 2.3	5	Aromatic cycle (or cycle with π-bonds), projection of a hydrogen bond donor and three projections of a hydrogen bond acceptor	10.92	85.7

3. CONCLUSION

QSAR analysis and pharmacophore modeling of anti-inflammatory activity of substituted (pyrrole[1,2-*a*][1,2,4]triazino[2,3-*c*]quinazoline-5*a*-yl)carboxylic acids were performed. According to the results of QSAR analysis, two three-parameter equations were obtained for each model of experimental inflammation, and it was found that the activity depends mainly on the descriptors that determine the spatial coordinates of the molecule atoms in the selected conformation. Pharmacophore modeling has shown that carboxyl group at the 5a position of substituted (pyrrolo[1,2-*a*][1,2,4]triazino[2,3-*c*]quinazoline-5*a*-yl)carboxylic acids is potential participant in the formation of hydrogen bonds. And additional factors influencing the activity are withdrawing substituents, namely aromatic (fluorophenyl) cycle at the certain distance and oxygen at the 2nd position. The resulting models are characterized by high predictive power, and subsequently can be used for virtual screening of anti-inflammatory activity of this class of compounds. Results of *in silico* research give understating, that studied (pyrrole[1,2-*a*][1,2,4]triazino[2,3-*c*]quinazoline-5*a*-yl)carboxylic acids could undergo further modifications, such as replacement of triazino moiety by other azole cycle or removing of it , with preservation of oxygen atom at quinazoline core. This can remain main types of interactions with researched bio-target observed at pharmacophore models. So, this is going be tested in our further work.

4. MATERIALS AND METHODS

4.1. Chemical part

To create QSAR and pharmacophore models, substituted 3-R-2,8-dioxo-7,8-dihydro-2*H*-pyrrolo[1,2-*a*][1,2,4]triazino[2,3-*c*]quinazoline-5*a*(6*H*)-yl)carboxylic (propanoic) acids and their esters were selected. Their synthesis and anti-inflammatory activity was described earlier [17, 18, 22] and shown in Figure 6 and Table 6.

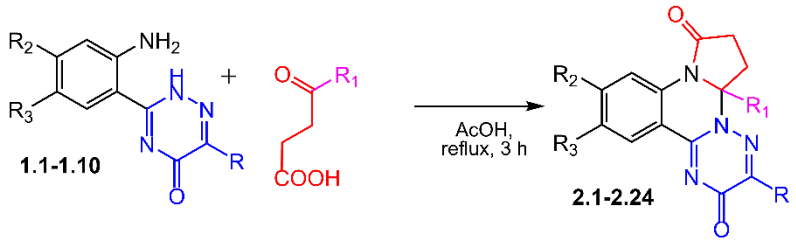

2.1 R=Me, R_1 = -COOH, R_2=R_3=H; **2.2** R=Ph, R_1=-COOH, R_2=R_3=H; **2.3** R=Ph, R_1=-COOH, R_2=F, R_3=H; **2.4** R=Ph, R_1=-COOH, R_2=H, R_3=F; **2.5** R=Ph, R_1=-COOH, R_2=R_3=F; **2.6** R=Ph, R_1=-COOH, R_2=H, R_3=Cl; **2.7** R=Ph, R_1=-COOH, R_2=H, R_3=Br; **2.8** R= 4-*i*-PrC_6H_4, R_1=-COOH, R_2=R_3=H, **2.9** R= 4-FC_6H_4, R_1=-COOH, R_2=R_3=H; **2.10** R= 4-FC_6H_4, R_1=-COOH, R_2=F, R_3=H; **2.11** R= 4-FC_6H_4, R_1=-COOH, R_2=H, R_3=F; **2.12** R= 4-FC_6H_4, R_1=-COOH, R_2=R_3=F; **2.13** R= Me, R_1=-$(CH_2)_2$COOH, R_2=R_3=H; **2.14** R=Ph, R_1=-$(CH_2)_2$COOH, R_2=R_3=H; **2.15** R=Ph, R_1=-$(CH_2)_2$COOH, R_2=F, R_3=H; **2.16** R=Ph, R_1=-$(CH_2)_2$COOH, R_2=H, H_3=F; **2.17** R=Ph, R_1=-$CH_2)_2$COOH, R_2=R_3=F; **2.18** R= 4-FC_6H_4, R_1=-$(CH_2)_2$COOH, R_2=R_3=H; **2.19** R= 4-FC_6H_4, R_1=-$(CH_2)_2$COOH, R_2=F, R_3=H; **2.20** R= 4-FC_6H_4, R_1=-()$CH_2)_2$COOH, R_2=H, R_3=F; **2.21** R= 4-FC_6H_4, R_1=-$(CH_2)_2$COOH, R_2=R_3=F; **2.22** R=Me, R_1=-COOEt, R_2=R_3=H; **2.23** R= Me, R_1=-$(CH_2)_2$COOEt, R_2=R_3= H; **2.24** R= 4-FC_6H_4, R_1=-$(CH_2)_2$COOEt, R_2=H, R_3=F

Figure 6 Approaches for the synthesis of 3-R-2,8-dioxo-7,8-dihydro-2*H*-pyrrolo[1,2-*a*][1,2,4]triazino[2,3-*c*]quinazoline-5*a*(6*H*)-yl)carboxylic (propanoic) acids and their esters.

Table 6. Anti-inflammatory activity (AA) of the synthesized compounds at 4 hours after inflammation induction (M±m. n=6)

Compound	R	R_1	R_2	R_3	AA, % (CE)[a]	AA, % (FE)[b]
Diclofenac	-	-	-	-	58.90	50.93-
2.1	Me	-COOH	H	H	57.90	53.76
2.2	Ph	-COOH	H	H	40.81	70.18
2.3	Ph	-COOH	F	H	75.77	59.52
2.4	Ph	-COOH	H	F	64.72	49.42
2.5	Ph	-COOH	F	F	54.92	46.74
2.6	Ph	-COOH	H	Cl	63.80	46.01
2.7	Ph	-COOH	H	Br	58.54	45.93
2.8	*i*-PrC_6H_4	-COOH	H	H	44.66	34.60
2.9	4-FC_6H_4	-COOH	H	H	63.02	64.30
2.10	4-FC_6H_4	-COOH	F	H	74.60	60.31
2.11	4-FC_6H_4	-COOH	H	F	69.23	64.38
2.12	4-FC_6H_4	-COOH	F	F	51.37	46.21
2.13	Me	-$(CH_2)_2$COOH	H	H	81.46	84.05
2.14	Ph	-$(CH_2)_2$COOH	H	H	50.40	32.33
2.15	Ph	-$(CH_2)_2$COOH	F	H	50.27	61.73
2.16	Ph	-$(CH_2)_2$COOH	H	F	60.46	42.69
2.17	Ph	-$(CH_2)_2$COOH	F	F	49.95	43.19
2.18	4-FC_6H_4	-$(CH_2)_2$COOH	H	H	69.15	82.98
2.19	4-FC_6H_4	-$(CH_2)_2$COOH	F	H	63.25	54.33
2.20	4-FC_6H_4	-$(CH_2)_2$COOH	H	F	53.85	50.78
2.21	4-FC_6H_4	-$(CH_2)_2$COOH	F	F	79.66	79.05
2.22	Me	COOEt	H	H	15.17	23.60
2.23	Me	-$(CH_2)_2$COEt	H	H	8.15	11.93
2.24	4-FC_6H_4	-$(CH_2)_2$COEt	–	F	16.91	19.84

[a] anti-inflammatory activity of «Carrageenan edema».
[b] anti-inflammatory activity of «Formalin edema».

4.2. QSAR-models

Optimized files of compounds were used for calculations of descriptors for QSAR. The following software was used: Dragon [23, 24], MOPAC2012 [25]. The correlation coefficients for all pair of descriptor variables used in the models were evaluated to identify highly correlated descriptors in order to detect redundancy in the data set. Hence, descriptors with constant variables and near-constant variables were excluded from the further consideration ($r \geq 0.95$). 1353 descriptors (22 blocks) were calculated for construction of QSAR-models, namely constitutional descriptors, topological descriptors, walk and path counts, connectivity indices, information indices, 2D autocorrelations, edge adjacency indices, Burden eigenvalues, topological charge indices, eigenvalue-based indices, Randic molecular profiles, geometrical descriptors, RDF descriptors, 3D-MoRSE descriptors, WHIM descriptors, GETAWAY descriptors, functional group counts, atom-centred fragments, charge descriptors, molecular properties, 2D binary fingerprints [26, 27], as well as descriptors were used experimental data on the anti-inflammatory activity of compounds (Table 6) [28, 29].

The multiple linear regression analysis based on genetic algorithm until 3 variants was applied to obtain the best descriptors among 1353 calculated overall, and to construct QSAR models using the QSARINS 2.2.4 [26]. The division into training and prediction sets was performed at a ratio of 80 to 20 percent relatively. Namely, 18 compounds were used for training set and 6 for prediction set. More detailed procedure of QSAR modeling was written at our previous study [27].

4.3. Pharmacophoric models

To model the pharmacophore responsible for the manifestation of the anti-inflammatory effect, we have used the program in the field of chemoinformatics Molecular Operating Environment (MOE) version 2007.09 [30-32]. The initial three-dimensional geometry of molecular structures was obtained by the method of molecular mechanics using the force field MMFF94x at an optimization gradient value of 0.01 kcal/mol. The next step was to create a base of conformers for each of the studied structures using stochastic search. Conformers with an internal energy that differs from the internal energy of the optimal structure for this compound by more than 7 kcal/mol were identified as energetically unstable and removed from the pharmacophore search process. For each conformer, the coordinates of potential pharmacophore centers were

generated: hydrophobic regions, donors and acceptors of hydrogen bonds (and their projections), aromatic cycles, and so on. Automatic search for pharmacophore models was performed by gradually increasing the number of pharmacophore centers required to discriminate between active and inactive compounds. The criterion for selecting the pharmacophore model was the accuracy of classification of compounds into active and inactive. Compounds that showed an activity level of at least 90% of the activity of the reference compound *in vivo* experiment were considered active, while others were considered inactive or insufficiently active (Table 6).

In addition to the accuracy of the model, we also analyzed such parameter as the degree of mutual overlap of active compounds. The higher the value of this indicator, the greater the spatial coincidence of the conformations of the active compounds, and the more there was reason to believe that the binding of active compounds to biotargeting takes place in the same way.

Acknowledgements: The work was carried out on the budgetary theme of the Ministry of Health of Ukraine «Design and synthesis of condensed pyrimidines and elaboration of based on them potential medications with anti-inflammatory, neurotropic and metabotropic activity» (period of study 2022-2024).

Author contributions: Concept – S.K.; Design – O.V.; Supervision – S.K.; Resources – O.D., O.A., Materials – V.S.; Data Collection and/or Processing – O.A., O.D.; Analysis and/or Interpretation – O.V.; Literature Search – O.V., S.K.; Writing – O.A., V.S.; Critical Reviews – V.S., O.A., O.D., O.V., S.K.

Conflict of interest statement: The authors declare that they have no conflict of interest.

REFERENCES

[1] Ajani OO, Audu OY, Aderohunmu DV, Owolabi FE, Olomieja AO. Undeniable pharmacological potentials of quinazoline motifs in therapeutic medicine. Am J Drug Discov Dev. 2017; 7: 1-24. [CrossRef]

[2] Reddy AG, Babu VH, Prakash RYJ. A review on quinazolines as anticancer agents. J Chem Pharm Sci. 2017; 10(3): 1492-1504. [CrossRef]

[3] Shagufta IA. An insight into the therapeutic potential of quinazoline derivatives as anticancer agents. Med Chem Commun. 2017; 8: 871-885. [CrossRef]

[4] Hameed A, al-Rashida M, Uroos M, Ali SA, Ishtiaq AM, Khan KM. Quinazoline and quinazolinone as important medicinal scaffoldes: a comparative patent review (2011-2016). Expert Opin Ther Pat. 2018; 4: 281-297. [CrossRef]

[5] Auti PS, George G, Paul AT. Recent advances in the pharmacological diversification of quinazoline/quinazolinone hybrids. RSC Adv. 2020; 10(68): 41353-41392. [CrossRef]

[6] Hameed A, Al-Rashida M, Uroos M, Ali SA, Arshia IM, Khan KM. Quinazoline and quinazolinone as important medicinal scaffolds: a comparative patent review (2011-2016). Expert Opin Ther Pat. 2018; 28(4): 281-297. [CrossRef]

[7] Ravez S, Castillo-Aguilera O, Depreux P, Goossens L. Quinazoline derivatives as anticancer drugs: a patent review (2011 - present). Expert Opin Ther Pat. 2015; 25(7): 1-16. [CrossRef]

[8] Li SN, Li HQ. Epidermal growth factor receptor inhibitors: a patent review (2010 - present). Expert Opin Ther Pat. 2014; 24(3): 309-21. [CrossRef]

[9] Marzaro G, Guiotto A, Chilin A. Quinazoline derivatives as potential anticancer agents: a patent review (2007 - 2010). Expert Opin Ther Pat. 2012; 22(3): 223-252. [CrossRef]

[10] Ismail RSM, Ismail NSM, Abuserii S, Abou El EDA. Recent advances in 4-aminoquinazoline based scaffold derivatives targeting EGFR kinases as anticancer agents. Future J Pharm Sci. 2016; 2(1): 9-19. [CrossRef]

[11] Alam J, Alam O, Naim MJ, Alam P. A review: recent investigations on quinazoline scaffold. Int J Adv Res. 2015; 3(12): 1656-1664. [CrossRef]

[12] Selvam TP, Kumar PV. Quinazoline marketed drugs – a review. Res Pharm. 2011; 1(1): 1-21. [CrossRef]

[13] Jafari E, Khajouei MR, Hassanzadeh F, Hakimelahi GH, Khodarahmi GA. Quinazolinone and quinazoline derivatives: recent structures with potent antimicrobial and cytotoxic activities. Res Pharm Sci. 2016; 11(1): 1-14. [CrossRef]

[14] Drugbank Online. https://go.drugbank.com/ (accessed 17 January 2022)

[15] Paul D, Sanap G, Shenoy S, Kalyane D, Kiran K, Tekade RK. Artificial intelligence in drug discovery and development. Drug Discov Today. 2021; 26(1): 80-93. [CrossRef]

[16] Talha B. A new paradigm for drug development. The Lancet Digit Health. 2020; 2(5): e226-e227. [CrossRef]

[17] Stavytskyi V, Antypenko O, Nosylenko I, Berest G, Voskoboinik O, Kovalenko S. Substituted 3-R-2,8-Dioxo-7,8-dihydro-2*H*-pyrrolo[1,2-*a*][1,2,4]triazino[2,3-*c*]quinazoline-5*a*(6*H*)-carboxylic acids and their salts – a promising class of anti-inflammatory agents. Antiinflamm Antiallergy Agents Med Chem. 2021; 20(1): 75-88. [CrossRef]

[18] Stavitsky VV, Voskoboinik OY, Kazunin MS, Nosylenko IS, Shishkina SV, Kovalenko SI. Substituted pyrrolo[1,2-*a*][1,2,4]triazolo-([1,2,4]triazino-)[*c*]quinazoline-4*a*(5*a*)-propanoic acids: synthesis, spectral characteristics and anti-inflammatory activity. Voprosy khimii i khimicheskoi tekhnologii. 2020; 1: 61-70. [CrossRef]

[19] Sidhu RS, Lee JY, Yuan C, Smith WL. Comparison of cyclooxygenase-1 crystal structures: cross-talk between monomers comprising cyclooxygenase-1 homodimers. Biochemistry. 2010; 49: 7069-7079. [CrossRef]

[20] Rowlinson SW, Kiefer JR, Prusakiewicz JJ, Pawlitz JL, Kozak KR, Kalgutkar AS, Stallings WC, Kurumbail RG, Marnett LJ. A novel mechanism of cyclooxygenase-2 inhibition involving interactions with Ser-530 and Tyr-385. J Biol Chem, 2003; 278(46): 45763-45769. [CrossRef]

[21] Auffinger P, Hays FA, Westhof E, Ho PS. Halogen bonds in biological molecules. Proc Natl Acad Sci. 2004; 101(48): 16789-16794. [CrossRef]

[22] Stavytskyi V, Voskoboinik O, Antypenko O, Krasovska N, Shabelnyk K, Konovalova I, Shishkyna S, Kholodniak S, Kovalenko S. Tandem heterocyclization of 2-(azolyl-(azinyl-))anilines as an efficient method for preparation of substituted pyrrolo[1,2-*a*]azolo-(azino-)[*c*]quinazolines. J Heterocyclic Chem. 2020; 57(3): 1249-1260. [CrossRef]

[23] Todeschini R, Consonni V, Handbook of Molecular Descriptors Wiley-VCH: Weinheim and New York, USA 2000.

[24] Talete srl DRAGON for Windows. (Software for Molecular Descriptor Calculations). Version 5.5–2007. http://www.talete.mi.it/ (accessed 17 January 2022).

[25] MOPAC2012. http://openmopac.net/MOPAC2012.html (accessed 17 January 2022)

[26] Gramatica P, Chirico N, Papa E, Cassani S, Kovarich S. QSARINS: A new software for the development, analysis, and validation of QSAR MLR models. J Comput Chem. 2013; 34: 2121-2132. [CrossRef]

[27] Antypenko OM, Kovalenko SI, Karpenko OV, Nikitin VO, Antypenko LM. Synthesis, anticancer, and QSAR studies of 2-alkyl(aryl,hetaryl)quinazolin-4(3*H*)-thione's and [1,2,4]triazolo[1,5-*c*]quinazoline-2-thione's thioderivatives. Helv Chim Acta. 2016; 99(8): 621-631. [CrossRef]

[28] Stavytskyi VV, Nosulenko IS, Portna OO, Shvets VM, Voskoboynik OYu, Kovalenko SI. Substituted pyrrolo[1,2-*a*][1,2,4]triazolo-(triazino-)[*c*]quinazolines - a promising class of lipoxygenase inhibitors. Curr Issues Pharm Med Sci Pract. 2020; 13(1): 4-10. [CrossRef]

[29] Krasovska NI, Stavytskyi VV, Nosulenko I, Kholodniak OV, Antypenko OM, Voskoboinik OYu, Kovalenko SI. Pyrrolo[1,2-*a*]azolo-(azino-)[*c*]quinazolines and their derivatives as 15-LOX inhibitors: design, *in vitro* studies and QSAR-analysis. J Res Pharm. 2021; 25(5): 1-9. [CrossRef]

[30] Yang SY. Pharmacophore modeling and applications in drug discovery: challenges and recent advances. Drug Discov Today. 2010; 15(11-12): 444-450. [CrossRef]

[31] Gao Q, Yang L, Zhu Y. Pharmacophore based drug design approach as a practical process in drug discovery. Curr Comput-Aid Drug. 2010; 6(1): 37-49. [CrossRef]

[32] Horvath D. Pharmacophore-based virtual screening. Methods in Molecular Biology. 2010, pp. 261-298. [CrossRef]